AGU PUBLICATIONS

Geophysical Research Letters

RESEARCH LETTER
10.1002/2015GL063299

Key Points:
- Heat content change dominated by heat transport convergence
- Due to widespread sinking trend of midthermocline isopycnals over 50+ years

Supporting Information:
- Figures S1–S2

Correspondence to:
S. Häkkinen,
sirpa.hakkinen@nasa.gov

Citation:
Häkkinen, S., P. B. Rhines, and D. L. Worthen (2015), Heat content variability in the North Atlantic Ocean in ocean reanalyses, *Geophys. Res. Lett.*, *42*, 2901–2909, doi:10.1002/2015GL063299.

Received 28 JAN 2015
Accepted 27 MAR 2015
Accepted article online 31 MAR 2015
Published online 22 APR 2015

Heat content variability in the North Atlantic Ocean in ocean reanalyses

Sirpa Häkkinen[1], Peter B. Rhines[2], and Denise L. Worthen[1,3]

[1]NASA Goddard Space Flight Center, Greenbelt, Maryland, USA, [2]University of Washington, Seattle, Washington, USA, [3]Wyle STE Group, Houston, Texas, USA

Abstract Warming of the North Atlantic Ocean from the 1950s to 2012 is analyzed on neutral density surfaces and vertical levels in the upper 2000 m. Three reanalyses and two observational data sets are compared. The net gain of 5×10^{22} J in the upper 2000 m is roughly 30% of the global ocean warming over this period. Upper ocean heat content (OHC) is dominated in most regions by heat transport convergence without widespread changes in the potential temperature/salinity relation. The heat convergence is associated with sinking of midthermocline isopycnals, with maximum sinking occurring at potential densities $\sigma_0 = 26.4-27.3$, which contain subtropical mode waters. Water masses lighter than $\sigma_0 = 27.3$ accumulate heat by increasing their volume, while heavier waters lose heat by decreasing their volume. Spatially, the OHC trend is nonuniform: the low latitudes, 0–30°N are warming steadily while large multidecadal variability occurs at latitudes 30–65°N.

1. Introduction

Studies of ocean heat content (OHC) show warming of the global oceans over the last 60 years. The OHC variability is significant globally and thought to represent some 93% of the heating of the Earth over the past 60 years [*Levitus et al.*, 2000, 2012; *Abraham et al.*, 2013]. The North Atlantic contribution is roughly 30% of the 50 year global OHC trend; together, the North and South Atlantic are thought to account for about 50% of the global trend. *Levitus et al.* [2012] attribute the trend to global warming, with the subtropical enhancement caused by uneven distribution of the warming. Global analysis of the trend 1950 to 2008 by *Durack and Wijffels* [2010] shows a dominating freshening (cooling) in the North Pacific but salinization (warming) of the subtropics in the upper 500 m in the North Atlantic. They argue that the migration of density surfaces is an important component of the salinity trends. Other studies, e.g., *Lozier et al.* [2008] show the warming occurring mainly in the subtropics but cooling in the subpolar gyre. They attribute this long-term trend from 1950–1970 to 1980–2000 to the North Atlantic Oscillation (NAO) while noting that the global warming signal is not obvious in their analysis. *Williams et al.* [2014] continued this work to separate temporal and spatial structure of the North Atlantic OHC into Ekman and Atlantic meridional overturning circulation (AMOC) contributions. They show that OHC anomalies in the subtropical and subpolar gyres are dominated by heat transport convergence.

There is significant decadal variability in OHC, which complicates the view of a simple linear trend, and this makes discussion of mechanisms and pathways of warming difficult. The most recent decade has seen the global warming signal (from surface air temperatures) undergoing a hiatus, which has been explained by some authors as increased uptake of heat by the deep ocean [*Meehl et al.*, 2011; *Balmaseda et al.*, 2013a; *Kosaka and Xie*, 2013; *England et al.*, 2014]. These authors attribute the hiatus to La Niña and Pacific decadal variability enhancing subduction of warm waters and upwelling of cold waters, but the Atlantic Ocean also shows similar behavior of increased deep ocean heat uptake during hiatus periods [*Meehl et al.*, 2011; *Balmaseda et al.*, 2013a].

Several studies argue why the North Atlantic displays the largest localized warming. One possibility is the internal dynamics related to the AMOC. *Palmer et al.* [2007] analyzed observations to derive heat content above the 14°C isotherm. They observe an increased heat convergence in the Atlantic sector which is compensated by heat divergence elsewhere. This leads them to suggest increased AMOC as the cause of enhanced increase of OHC in the Atlantic. A model study of *Grist et al.* [2010] shows a dominant contribution of AMOC to OHC variability in the upper 500 m across the North Atlantic extending to 30°S. Also, *Lee et al.* [2011] have suggested based on numerical simulation that increased South Atlantic MOC and increased Agulhas leakage have made the North Atlantic warming trend larger than in any other basin.

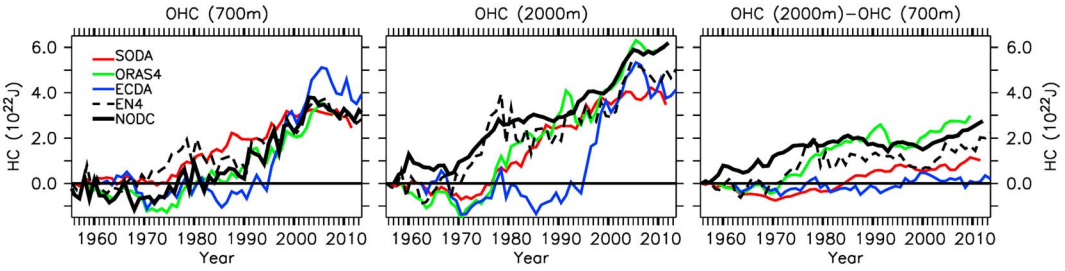

Figure 1. Evolution of the North Atlantic (0–65°N) heat content anomaly integrated over upper 700 m, 2000 m, and their difference for the reanalyses SODA, ORAS4, ECDA, and data reconstructions EN4 and NODC. Colors denote different data sets labeled in the left figure. All are referenced to the first year of the record. Units are 10^{22} J.

We consider aspects of the North Atlantic warming in the top 700 m and 2000 m of the water column. We will explore the role of vertical migration of isopycnal surfaces ("heaving"), which turns out to have a dominant role in the upper ocean heat content changes. This investigation uses the approach of *Bindoff and McDougall* [1994] to define heat content change in terms of isopycnal heaving and water mass formation contributions. However, we emphasize that "heaving" does not necessarily imply adiabatic vertical movement of waters forced, for example, by changes in atmospheric winds. Heaving of isopycnals can also arise from changes in the rate of water mass renewal. Changes in the temperature and salinity contributions to the density can occur for many reasons, notably atmospheric heat and fresh water flux, and these may or may not conform to the θ/S relation of the prior ocean state.

2. Data

The data sets used are ocean state estimates from Simple Ocean Data Assimilation (SODA) [*Carton and Giese*, 2008], the operational ocean reanalysis system by European Centre for Medium-Range Weather Forecasts (ORAS4) [*Balmaseda et al.*, 2013b], and a National Oceanic and Atmospheric Administration (NOAA)/Geophysical Fluid Dynamics Laboratory reanalysis product (ECDA) [*Zhang et al.*, 2007; *Chang et al.*, 2013]. Observational OHC data for the top 700 and 2000 m were retrieved from the National Oceanographic Data Center (NODC) archive [*Levitus et al.*, 2012]. The 700 m OHC data are available as annual averages 1955–2011, while the 2000 m data are pentadal averages interpolated to an annual data set, 1957–2009. We also use an objectively analyzed hydrographic data set, EN4.0.2, from the UK Met Office [*Good et al.*, 2013] with 1° resolution, from 1948 to present. SODA (version 2.2.8 ensemble mean) covers years 1955–2011, ORAS4 1958–2013, and ECDA 1961–2009. The spatial resolutions are 0.5° for SODA, and 1° for ORAS4 and ECDA (with a finer resolution in tropics); all are monthly data. For each data set, except NODC (has only pentadal salinity data before 2005 and annual temperature anomalies limited to top 700 m), we compile annual temperature, salinity data, and potential density (σ_0). OHCs are computed in the original grid at annual resolution. We also compute the neutral density values for each reanalysis and EN4 (uses temperature, salinity, and horizontal and vertical grid location) based on algorithms of *Jackett and McDougall* [1997] (from http://www.teos-10.org/preteos10_software/neutral_density.html).

3. Results

3.1. Ocean Heat Content

The integrated 0–700 and 0–2000 m heat content from the reanalysis data sets is compared with NODC data and shown in Figure 1. The heat content anomaly is summed for the region 0–65°N, including the Gulf of Mexico and excluding the Mediterranean. Figure 1 shows that SODA and ORAS4 capture the observed amplitude of OHC change for the 0–700 m column, where the observational data coverage should be the best. However, the observed data sets differ in detail as in the period 1970–1990, when EN4 OHC is warmer than NODC. In the case of 0–2000 m OHC, all reanalyses are colder than observations in the early years but SODA and ORAS4 lie closer to observations after 1985. Deep OHC 700 m–2000 m, in Figure 1, displays a considerable spread in the upward trend among all data sets and also between the two observational data sets. Here ECDA is the outlier with no significant deep warming trend. Presumably, these reanalyses are using mostly the same observations, but Figure 1 results show their differing success

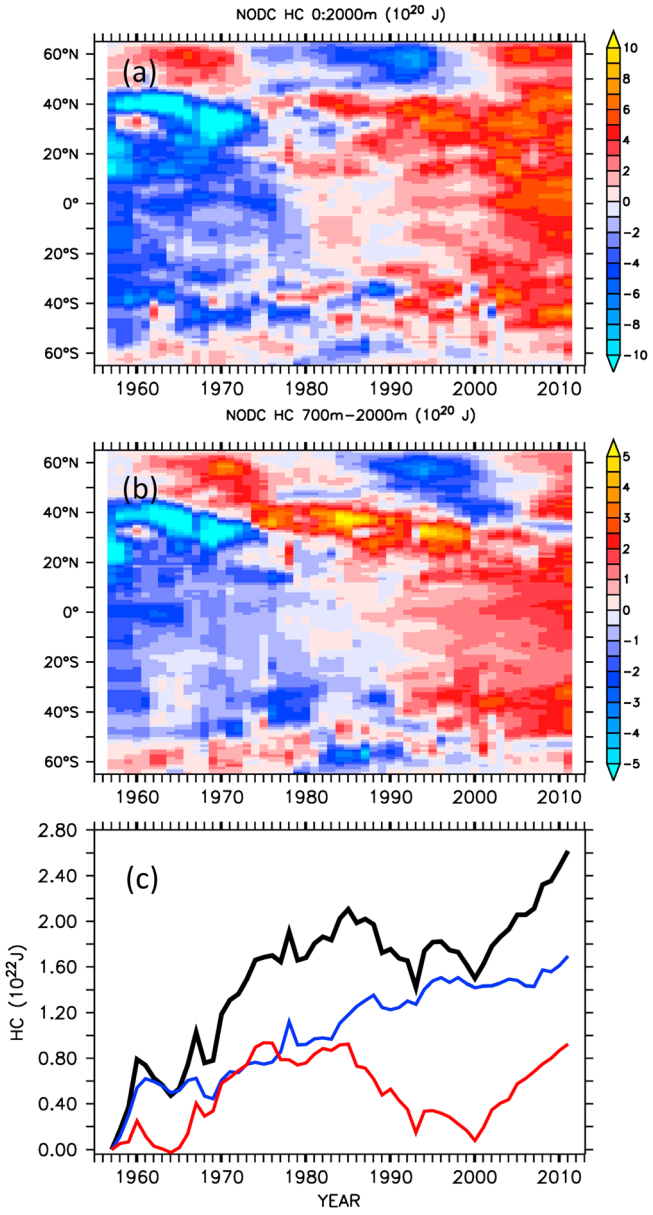

Figure 2. Evolution of NODC zonal sum OHC in the Atlantic 65°S–65°N integrated over (a) 0–2000 m and (b) 700–2000 m. OHC units of 10^{20} J per degree of latitude. (c) Heat content integrated over 700–2000 m; 0–65°N (black), 0–30°N (blue), and 30–65°N (red) in units of 10^{22} J (referenced to the year 1955).

in constraining the deep heat content trend in comparison with NODC or EN4 observations. Also, the observational data sets would benefit from scrutiny as the OHC differences in Figure 1 indicate. *Durack et al.* [2014] suggest that undersampling before the modern era has led to widespread underestimates of ocean warming.

To examine the OHC latitudinal evolution the zonal average OHC in the whole Atlantic sector is shown in Figure 2a for the NODC 0–2000 m OHC. North of 50°N OHC anomalies, cold 1970–1995, warm before 1970 and after 1995, represent Atlantic Multidecadal Variability (or "Atlantic Multidecadal Oscillation," AMO) [*Enfield et al.*, 2001]. The rest of the Atlantic OHC display in-phase variability on both hemispheres, suggesting a common forcing, such as AMOC [e.g., *Grist et al.*, 2010]. (In SODA, ORAS4, and ECDA not shown here, the evolution is similar.) In middepth (700–2000 m) OHC, Figure 2b, the southward propagation of anomalies associated with AMO away from the northern subpolar gyre is highly

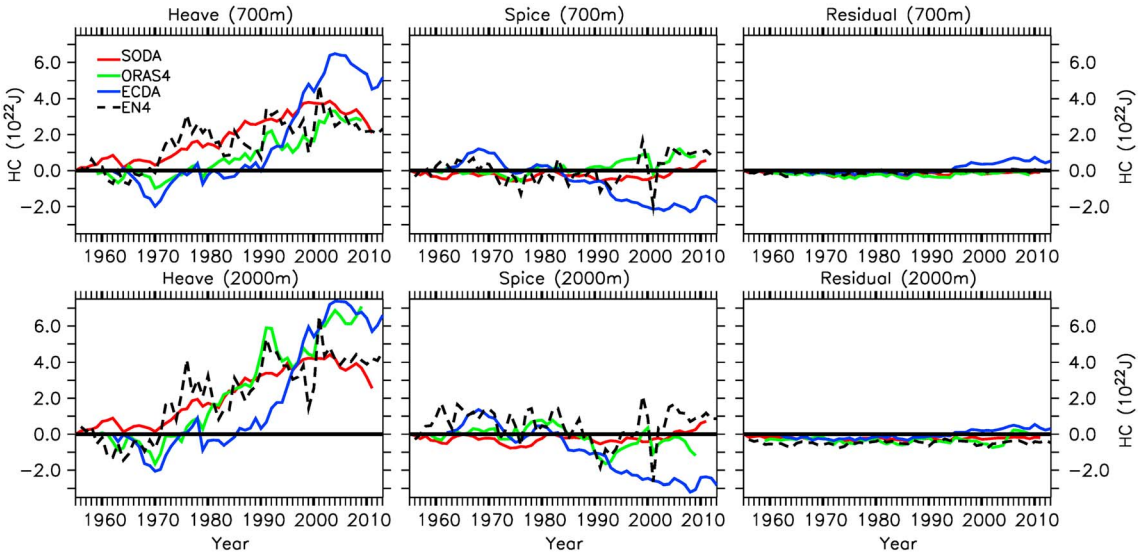

Figure 3. OHC 0–700 m and 0–2000 m time series for heaving, water mass change, and residual components in units of 10^{22} J. Colors denote different data sets (SODA, ORAS4, ECDA, and objectively analyzed data, EN4) labeled in the top left figure. All are referenced to the first year of the record.

distinguishable. Dividing OHC into two regions based on AMO impact (in Figure 2b) suggests that AMO-associated anomalies at latitudes 30–65°N are responsible for the steep increase in the deep (700–2000 m) OHC since year 2000 (Figure 2c), while OHC in the region 0–30°N has increased steadily (also seen in 0–2000 m OHC; Figure S1 in the supporting information).

3.2. Heat Content Trend due to Heaving and Water Mass Change

To separate OHC contributions due to isopycnal heaving and water mass change we adopt an approach of *Bindoff and McDougall* [1994]. In each grid point potential temperature (θ) change is divided into a change along the neutral density surface and due to vertical movement of the neutral density surface (dz/dt) (positive downward):

$$d\theta/dt\,|_z = d\theta/dt\,|_n + dz/dt\,|_n d\theta/dz \quad (1)$$

The first term on the right is temperature (water mass) change anomaly on constant neutral density surfaces (due to changes of θ/S; S = salinity), known also as "spice". The second term is the "heaving". The heaving dominates the OHC trends as will be seen.

The 700 m and 2000 m OHCs, summing the right-hand side components of (1) multiplied by ρC_p and thickness and area at each grid point, are displayed in Figure 3 for the three reanalyses and EN4 (referenced to the first year of the reanalysis, 1955 for EN4). In all cases heaving dominates the OHC as isopycnals are displaced downward, while the spice plays a rather small role opposing the heaving in the total heat content change. SODA and ORAS4 appear to be the closest to EN4 observational estimates. The heaving and spice decomposition break down at or near the surface where new water masses form due to heating or cooling. A residual OHC term can be computed, and here we show its evolution also in Figure 3; the largest contribution coming from surface layer (<50 m; shown later in Figure 5b), but the residual OHC is an order of magnitude smaller than the OHC heave component.

To explore how the long-term changes in OHC components are distributed spatially in the 0–700 m layer (and 0–2000 m layer in Figure S2) we compute OHC difference based on 15 year periods, (1961–1975) and (1995–2009), which are common for all three reanalyses (Figure 4). Their difference expresses the spatial variability of the trend in OHC and its components while diminishing the role of the AMO, which is in the positive phase during those time periods. The subtropical water layer OHC change peaks along the Gulf Stream (and its recirculation gyres), and the North Atlantic Current in all three reanalyses and in EN4. Changes are mostly determined by the heaving component. SODA emphasizes vertical and lateral advection convergence in the NE Atlantic, while ORAS4 and ECDA have the main center of action over the Gulf

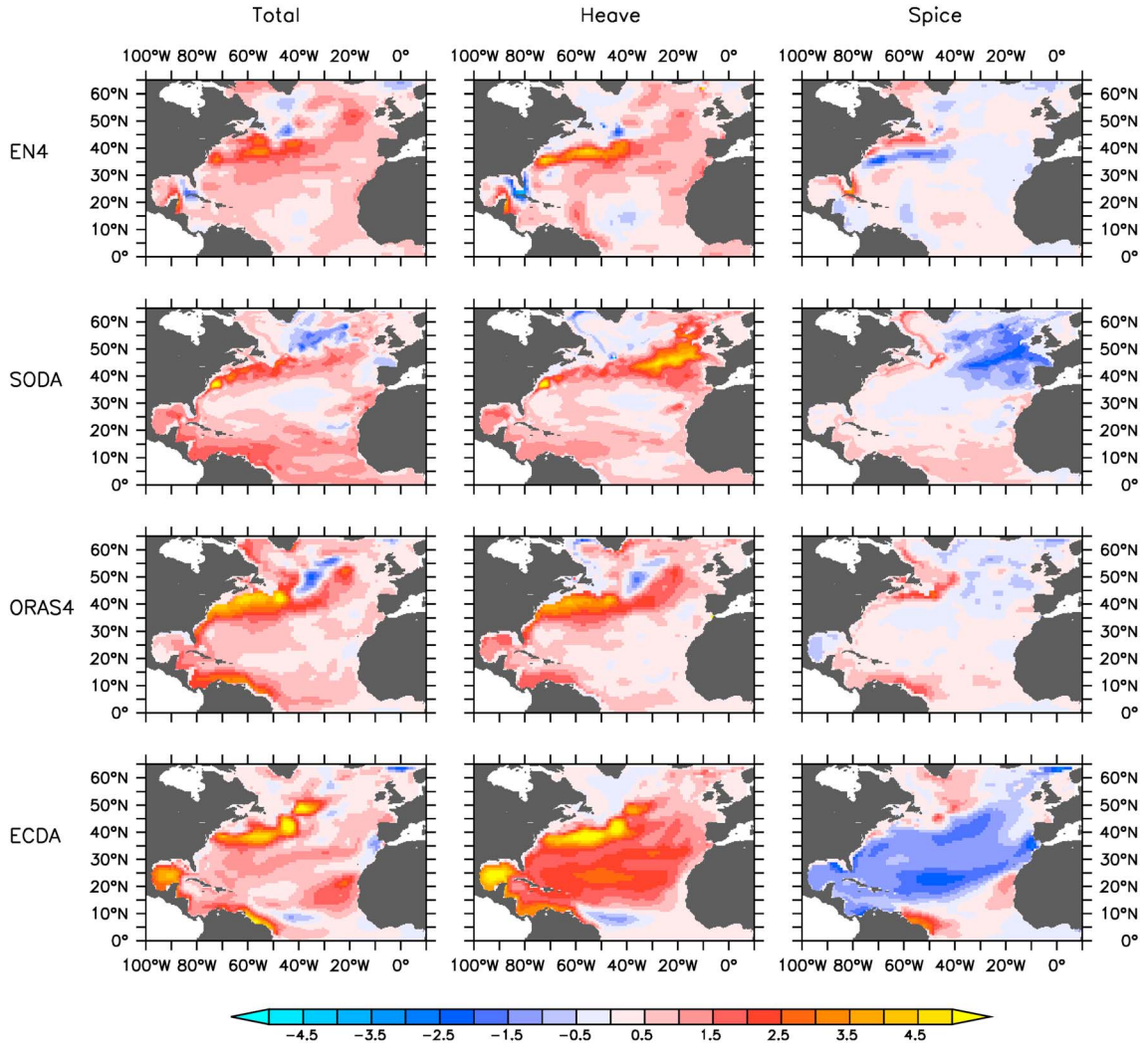

Figure 4. OHC change [1995:2009] − [1961:1975] integrated over 0–700 m and its components shown in the three reanalyses, SODA, ORAS4, and ECDA and objectively analyzed data, EN4. The units are $10^9 \mathrm{Jm}^{-2}$.

Stream-North Atlantic Current. SODA's center of action is in the subtropical/subpolar transition region where the North Atlantic Current experiences cooling, and downward Ekman pumping occurs. The cooling that dominates the subpolar gyre in some trend analyses is weakened by strong subpolar warming of the 2000s (clearly seen in Figure 2a). Water mass ("spice") change components differ significantly from each other in all reanalyses while contributing modestly to the total OHC change.

3.3. Vertical Structure of Changes

Since heaving changes are so important, we compute isopycnal depth displacement (in σ_0 space) as area average for SODA, ORAS4, ECDA, and EN4 for the North Atlantic (Figure 5a) as decadal averages referenced to the first common decade, 1961–1970. After the second decade, depths of midthermocline isopycnals have steadily increased in all reanalyses and in the observational data. SODA and ORAS4 show slowing down on the recent decade. In SODA the largest deepening has occurred in the middepth isopycnals, $\sigma_0 = 26.8$–27.4, with a maximum at around $\sigma_0 = 27.0$–27.2 (Figure 5a). Peaking of the isopycnal deepening at around 27.0–27.2 creates thinning of the denser layers below but increasing layer thickness above. ECDA, ORAS4, and EN4 tend to have two local maxima in the deepening, one around 26.5, a central density of the 18°C water, and at 27.2–27.3, the lightest subpolar mode waters. In ECDA the deepening far exceeds the other data sets. Overall, these reanalyses demonstrate that the isopycnal deepening is strong

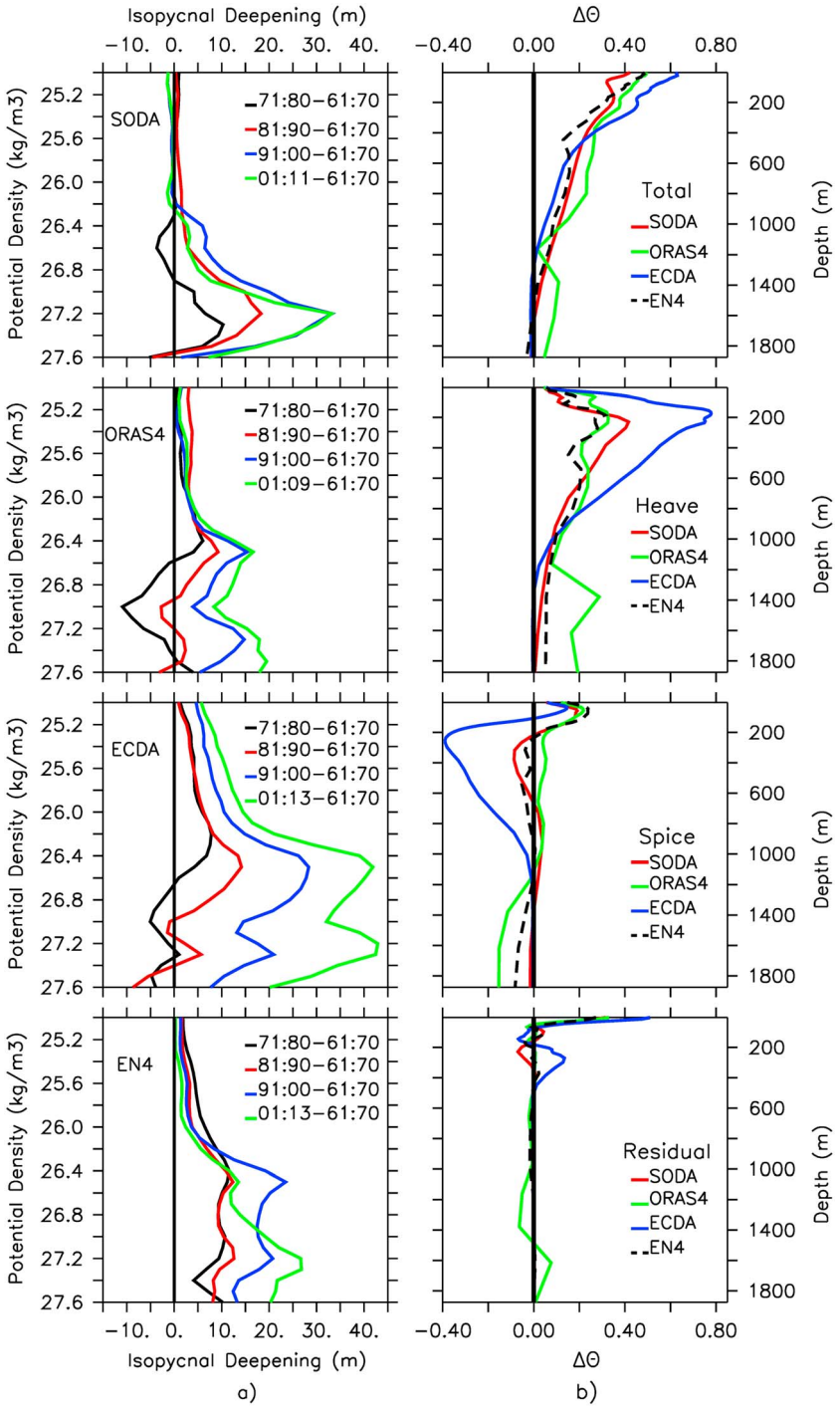

Figure 5. (a) Area average vertical migration of isopycnals in SODA, ORAS4, ECDA, and objectively analyzed data, EN4 in the North Atlantic in meters as decadal averages referenced to 1961–1970, positive values denote deepening, negative denote shoaling. (b) Potential temperature change [1995–2009] minus [1961–1975] versus depth in the same data sets: the total change, due to heaving and due to water mass change (spice), and residual, in units of Celsius.

even as basin averages. Previously, *Leadbetter et al.* [2007] and *Arbic and Owens* [2001] had identified the deepening trend of middepth isopycnals at a few hydrographic sections in the North Atlantic.

To show where the largest temperature changes due to heaving and spice occurred, we plot the area average temperature and their components versus depth as late minus early 15 year periods. Figure 5b shows the

largest warming in the upper ocean gradually diminishing downward, vanishing at 1500 m, except in ORAS4 which has a secondary warming at 1400 m–2000 m. Heaving contribution is largest around 200–300 m. Only ORAS4 has another maximum at 1400 m. In the spice component, surface heating gives away to subsurface cooling by 200 m depth. Overall, much more differences exist in this component with particularly strong cooling at depth in ORAS4. Figure 5b also shows that temperature changes below 1000 m are minimal (except in ORAS4); hence, the OHC trend in the layer 700 to 2000 m comes mostly from above the permanent pycnocline (~1200 m–1500 m) and not from the deep ocean. Figure 4b also shows the residual which is largest at the surface where the decomposition fails when a lighter water mass forms.

The observed, widespread descent of isopycnal surfaces and thickening of upper ocean isopycnal layers dynamically represent potential vorticity (PV) decline and increased OHC in major regions of the North Atlantic Ocean; potential vorticity, q, at scales larger than the Rossby deformation radius is dominated by $q \approx f\,\partial\sigma/\partial z$, where f is Coriolis frequency and $\partial\sigma/\partial z$ varies inversely with layer thickness. Production of low-PV mode waters can occur both by deep winter convection, ("cold subduction") and by "warm subduction" driven by Ekman pumping. The recurring pattern in Figure 5 shows PV extraction in the upper ocean with PV increase beneath (dividing at $\sigma_0 \approx 27.2$ in SODA and 26.4 in the other reanalyses and EN4 data). Lateral advection must account for the increase of PV in unventilated layers; while ventilated layers are subject to vertical subduction, water mass transformation, and lateral transport which all place bounds on the sources of the observed OHC variability. The concentrated OHC gain in the Gulf Stream-North Atlantic Current region is consistent with both air/sea heat flux and lateral advection, where the latter dominates.

4. Discussion

Three ocean reanalyses, SODA, ORAS4, and ECDA, are used to investigate the North Atlantic OHC. The three reanalyses and two observational data sets, NODC and EN4, all show significant disagreement as to amplitude and spatial patterns of OHC variability; however, all three reanalyses agree that the OHCs are to a high degree governed by heaving of isopycnals, particularly in the Gulf Stream-North Atlantic Currrent region. This reflects importance of heat transport convergence in creating OHC anomalies in the North Atlantic as found also by *Palmer et al*. [2007], *Palmer and Haines* [2009], and *Williams et al*. [2014]. Below 700 m, agreement among reanalyses is poor. This is particularly important in view of arguments suggesting that extensive deep ocean warming may compensate for the "hiatus" in global warming of surface air temperature since 2000 [*Balmaseda et al*., 2013a]. In the North Atlantic, all our reanalyses and objectively analyzed data show a hiatus with zero warming in 0–700 m during 2005–2013. Deeper warming (700–2000 m) does occur in the ORAS4 and SODA reanalysis and in NODC data but not elsewhere during this most recent period. It should be noted that deep warming can also result from changes in water mass renewal: subtropical mode waters are forming at the expense of deeper water masses.

We find widespread sinking of midthermocline isopycnals peaking at densities $\sigma_0 = 26.4$–27.3, at subtropical and subpolar mode water densities. This heaving can result from vertical or lateral processes of advection, mixing, and Ekman pumping but also from changes in water mass renewal. The sinking of isopycnals along 36 N between 1959 and 2005 was discussed by *Leadbetter et al*. [2007]. An even longer trend of sinking was discussed by *Arbic and Owens* [2001] along historical hydrographic sections. Leadbetter et al. considered the changes to be associated with Ekman pumping due to NAO fluctuations. However, heaving due to heat transport convergence can also originate from advection from outside the region. The concentrated OHC anomaly in the Gulf Stream/North Atlantic Current region suggests boundary current advection from the tropical Atlantic. AMOC as a potential cause of the heat content variability could involve the exchange across the equator as suggested by *Palmer et al*. [2007] and is seen in numerical hindcasts by *Lee et al*. [2011] and *Grist et al*. [2010]. Unfortunately, there is no agreement on AMOC evolution between available ocean reanalyses [*Pohlmann et al*., 2013; *Munoz et al*., 2011].

Our study and the aforementioned studies suggest that water mass variability ("spice") along isopycnals is less important in the thermocline and above. However, in regions with active deep convection, variation of the θ/S balance along isopycnals is known to occur. This may be the reason for the strong spice contribution in the northeast Atlantic in the SODA reanalysis (Figures 4), where Subpolar Mode Water is formed by wintertime convection. Interpretation of this trend is made difficult by AMO variability visible in Figure 2. In situ measurements during the Labrador Sea convection [e.g., *Lilly et al*., 1999] show large

"spice" variation as atmospheric cooling penetrates the buoyancy barrier, originating from the low-salinity West Greenland boundary current and reaching the more saline Irminger Current water. Interannual variability of the water masses in this region tends to involve larger excursions in θ and in S than in density, and this holds true, for example, with North Atlantic Deep Water far south of its origins, at 25 N [*Atkinson et al*., 2012].

Monitoring of the temperature and salinity transports at 26.5 N in the RAPID program [*Johns et al*., 2011] and study of the continuity of western boundary transports over large ranges of latitude [*Elipot et al*., 2014] are central to understanding the role of AMOC in OHC variability. Moreover, given the wide variety of amplitudes and space-time behavior of the reanalyses Atlantic OHC, and the small (10 m–20 m) vertical migration of isopyncal surfaces involved in OHC increase, continuing scrutiny of error in the NODC and EN4 data sets is also warranted.

Acknowledgments
We thank the NASA Ocean Surface Topography Program and the Physical Oceanography Program for support. We also want to thank the anonymous reviewers for their constructive criticism. All data are publicly available from the www.reanalysis.org website and from NOAA/NODC data center (downloaded February 2014). UK Met Office EN4.0.2 data set is available from www.metoffice.gov.uk/hadobs/en4.

The Editor thanks two anonymous reviewers for their assistance in evaluating this paper.

References

Abraham, J. P., et al. (2013), A review of global ocean temperature observations: Implications for ocean heat content estimates and climate change, *Rev. Geophys.*, *51*, 450–483, doi:10.1002/rog.20022.

Arbic, B. K., and W. B. Owens (2001), Climatic warming of Atlantic intermediate waters, *J. Clim.*, *14*, 4091–4108.

Atkinson, C. P., H. Bryden, S. Cunnigham, and B. King (2012), Atlantic transport variability at 25°N in six hydrographic sections, *Ocean Sci.*, *8*, 497–523, doi:10.5194/os-8-497-2012.

Balmaseda, M. A., K. E. Trenberth, and E. Källen (2013a), Distinctive climate signals in reanalysis of global ocean heat content, *Geophys. Res. Lett.*, *40*, 1754–1759, doi:10.1002/grl.50382.

Balmaseda, M. A., K. Morgensen, and A. T. Weaver (2013b), Evaluation of the ECMWF ocean reanalysis system ORAS4, *Q. J. R. Meteorol. Soc.*, *139*, 1132–1161.

Bindoff, N. L., and T. J. McDougall (1994), Diagnosing climate change and ocean ventilation using hydrographic data, *J. Phys. Oceanogr.*, *24*, 1137–1152.

Carton, J. A., and B. S. Giese (2008), A reanalysis of ocean climate using Simple Ocean Data Assimilation (SODA), *Mon. Weather Rev.*, *136*, 2999–3017.

Chang, Y.-S., S. Zhang, A. Rosati, T. L. Delworth, and W. F. Stern (2013), An assessment of oceanic variability for 1960–2010 from the ECDA ensemble coupled data assimilation, *Clim. Dyn.*, *40*(3–4), 775–803, doi:10.1007/s00382-012-1412-2.

Durack, P. J., and S. E. Wijffels (2010), Fifty-year trends in global ocean salinities and their relationship to broad-scale warming, *J. Clim.*, *23*, 4342–4362, doi:10.1175/2010JCLI3377.1.

Durack, P. J., P. Gleckler, F. Landerer, and K. Taylor (2014), Quantifying estimates of long-term global warming, *Nat. Clim. Change*, *4*, 999–1005, doi:10.1038/NCLIMATE2389.

Elipot, S., E. Frajka-Williams, C. Hughes, and J. Willis (2014), The observed North Atlantic meridional overturning circulation: Its meridional coherence and ocean bottom pressure, *J. Phys. Oceanogr.*, *44*, 517–537, doi:10.1175/JPO-D-13-026.1.

Enfield, D. B., A. M. Mestas-Nunez, and P. J. Trimble (2001), The Atlantic multidecadal oscillation and its relation to rainfall and river flows in the continental U.S., *Geophys. Res. Lett.*, *28*(10), 2077–2080, doi:10.1029/2000GL012745.

England, M. H., S. McGregor, P. Spence, G. A. Meehl, A. Timmermann, W. Cai, A. Sen Gupta, M. J. McPhaden, A. Purich, and A. Santoso (2014), Recent intensification of wind-driven circulation in the Pacific and the ongoing warming hiatus, *Nat. Clim. Change*, *4*, 222–227, doi:10.1038/NCLIMATE2106.

Good, S. A., M. J. Martin, and N. A. Rayner (2013), EN4: Quality controlled ocean temperature and salinity profiles and monthly objective analyses with uncertainty estimates, *J. Geophys. Res. Oceans*, *118*, 6704–6716, doi:10.1002/2013JC009067.

Grist, J. P., et al. (2010), The roles of surface heat flux and ocean heat transport convergence in determining Atlantic Ocean temperature variability, *Ocean Dyn.*, *60*, 771–790, doi:10.1007/s10236-010-0292-4.

Jackett, D. R., and T. McDougall (1997), A neutral density variable for the world's oceans, *J. Phys. Oceanogr.*, *27*, 237–263, doi:10.1175/1520-0485(1997)027<0237:ANDVFT>2.0.CO;2.

Johns, W. E., et al. (2011), Continuous, array-based estimates of Atlantic Ocean heat transport at 26.58 N, *J. Clim.*, *24*, 2429–2449, doi:10.1175/2010JCLI3997.1.

Kosaka, Y., and S.-P. Xie (2013), Recent global-warming hiatus tied to equatorial Pacific surface cooling, *Nature*, *501*, 403–407.

Leadbetter, S. J., R. G. Williams, E. L. McDonagh, and B. A. King (2007), A twenty year reversal in water mass trends in the subtropical North Atlantic, *Geophys. Res. Lett.*, *34*, L12608, doi:10.1029/2007GL029957.

Lee, S.-K., W. Park, E. van Sebille, M. O. Baringer, C. Wang, D. B. Enfield, S. G. Yeager, and B. P. Kirtman (2011), What caused the significant increase in Atlantic Ocean heat content since the mid-20th century?, *Geophys. Res. Lett.*, *38*, L17607, doi:10.1029/2011GL048856.

Levitus, S., J. Antonov, T. P. Boyer, and C. Stephens (2000), Warming of the world ocean, *Science*, *287*, 2225–2229, doi:10.1126/science.287.5461.2225.

Levitus, S., et al. (2012), World ocean heat content and thermosteric sea level change (0–2000 m), 1955–2010, *Geophys. Res. Lett.*, *39*, L10603, doi:10.1029/2012GL051106.

Lilly, J. M., P. B. Rhines, M. Visbeck, R. Davis, J. R. N. Lazier, F. Schott, and D. Farmer (1999), Observing deep convection in the Labrador Sea during winter 1994/95, *J. Phys. Oceanogr.*, *29*, 2065–2098.

Lozier, M. S., S. Leadbetter, R. G. Williams, V. Roussenov, M. S. Reed, and N. J. Moore (2008), The spatial pattern and mechanisms of heat content change in the North Atlantic, *Science*, *319*, 800–803.

Meehl, G. A., J. Arblaster, J. Fasullo, A. Hu, and K. Trenberth (2011), Model-based evidence of deep ocean heat uptake during surface temperature hiatus periods, *Nat. Clim. Change*, *1*, 360–364, doi:10.1038/NCLIMATE1229.

Munoz, E., B. Kirtman, and W. Weijer (2011), Varied representation of the Atlantic Meridional Overturning across multidecadal ocean reanalyses, *Deep Sea Res., Part II*, *58*, 1848–1857, doi:10.1016/j.dsr2.2010.10.064.

Palmer, M. D., and K. Haines (2009), Estimating oceanic heat content change using isotherms, *J. Clim.*, *22*, 4953–4969.

Palmer, M. D., K. Haines, S. F. B. Tett, and T. J. Ansell (2007), Isolating the signal of ocean global warming, *Geophys. Res. Lett.*, *34*, L23610, doi:10.1029/2007GL031712.

Pohlmann, H., D. M. Smith, M. A. Balmaseda, N. S. Keenlyside, S. Masina, D. Matei, W. A. Müller, and P. Rogel (2013), Predictability of the mid-latitude Atlantic meridional overturning circulation in a multi-model system, *Clim. Dyn.*, *41*, 775–785, doi:10.1007/s00382-013-1663-6.

Williams, R., V. Roussenov, D. Smith, and M. S. Lozier (2014), Decadal evolution of ocean thermal anomalies in the North Atlantic: The effects of Ekman, overturning, and horizontal transport, *J. Clim.*, *27*, 698–719, doi:10.1175/JCLI-D-12-00234.1.

Zhang, S., M. J. Harrison, A. Rosati, and A. T. Wittenberg (2007), System design and evaluation of coupled ensemble data assimilation for global oceanic climate studies, *Mon. Weather Rev.*, *135*, 3541–3564, doi:10.1175/MWR3466.1.